ACS APPLIED BIO MATERIALS

www.acsabm.org Letter

Fluorometric Determination of DNA Nanostructure Biostability

Hannah Talbot, Bharath Raj Madhanagopal, Andrew Hayden, Ken Halvorsen, and Arun Richard Chandrasekaran*

Cite This: https://doi.org/10.1021/acsabm.3c00287 Read Online

ACCESS | Metrics & More | Article Recommendations | Supporting Information

ABSTRACT: The analysis and improvement of DNA nanostructure biostability is one of the keys areas of progress needed in DNA nanotechnology applications. Here, we present a plate-compatible fluorometric assay for measuring DNA nanostructure biostability using the common intercalator ethidium bromide. We demonstrate the assay by testing the biostability of duplex DNA, a double crossover DNA motif, and a DNA origami nanostructure against different nucleases and in fetal bovine serum. This method scales well to measure a large number of samples using a plate reader and can complement existing methods for assessing and developing robust DNA nanostructures.

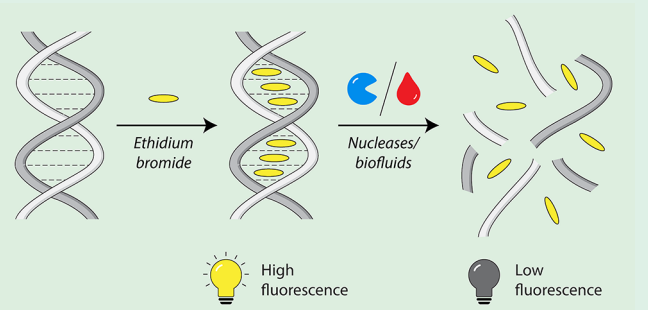

KEYWORDS: *DNA nanotechnology, biostability, nuclease degradation, DNA origami, DNA nanostructures*

Biostability is a key parameter for DNA nanostructures to be useful in biological applications.[1] Some of the strategies that have been developed to enhance the biostability of DNA nanostructures include chemical functionalization,[2,3] protective coatings,[4,5] addition of nuclease inhibitors,[6,7] and design-based strategies.[8,9] With improvements in biostability, different strategies have also been developed to analyze the degradation (and enhanced stability) of DNA nanostructures in physiological environments. These methods include gel-based analysis,[10] fluorescence,[11] light scattering,[12] atomic force microscopy (AFM),[13] and transmission electron microscopy (TEM).[14] Since AFM and TEM require specialized equipment and skilled personnel, gel-based analysis has been the most commonly used technique to analyze nuclease degradation. While gel electrophoresis is easy to adapt, readout takes >1 h and only for a limited number of samples per gel. Similarly, while fluorophore-based techniques are easy to design, there are costs associated with modifying component DNA strands with fluorophores. Size-exclusion chromatography methods developed for the purification of DNA nanostructures can also be used to monitor DNA nanostructure degradation, but require specific optimization protocols for different structures tested.[15,16] For various DNA nanostructures to be studied in different solution conditions, simpler and more scalable methods have to be developed. Working toward that, we report a fluorometric assay for analyzing DNA nanostructure biostability using the ubiquitous intercalator ethidium bromide (EBr). Once bound to DNA, EBr exhibits a 20- to 25-fold fluorescence enhancement, thereby making it useful as a DNA gel stain and as a fluorescent probe to study nucleic acid interactions.[17] In this biostability assay, EBr molecules bound to intact DNA nanostructures exhibit enhanced fluorescence, but upon degradation of the DNA nanostructures, the EBr molecules are released, which causes a reduction in fluorescence signal (Figure 1).

For our analysis, we chose the DNA double crossover (DX) motif as a model nanostructure (Figure 2a and Figure S1). The DX motif contains two adjacent double helical domains

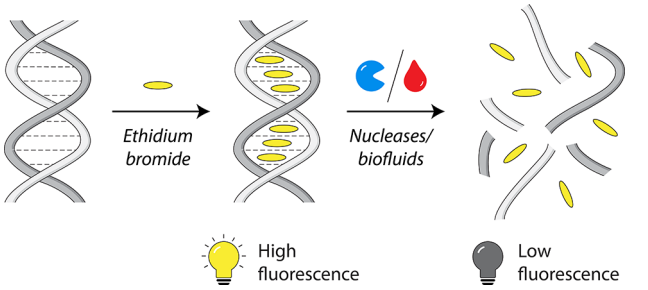

Figure 1. Overview of the assay. Fluorescent intercalators (e.g., ethidium bromide) show higher fluorescence when bound to double-stranded DNA or DNA nanostructures. Upon degradation by nucleases or in body fluids, the intercalators are released from the DNA nanostructures, which causes a reduction in the fluorescence signal. This signal off strategy can be used to monitor degradation profiles of DNA nanostructures.

Received: April 14, 2023
Accepted: May 30, 2023

https://doi.org/10.1021/acsabm.3c00287
ACS Appl. Bio Mater. XXXX, XXX, XXX−XXX

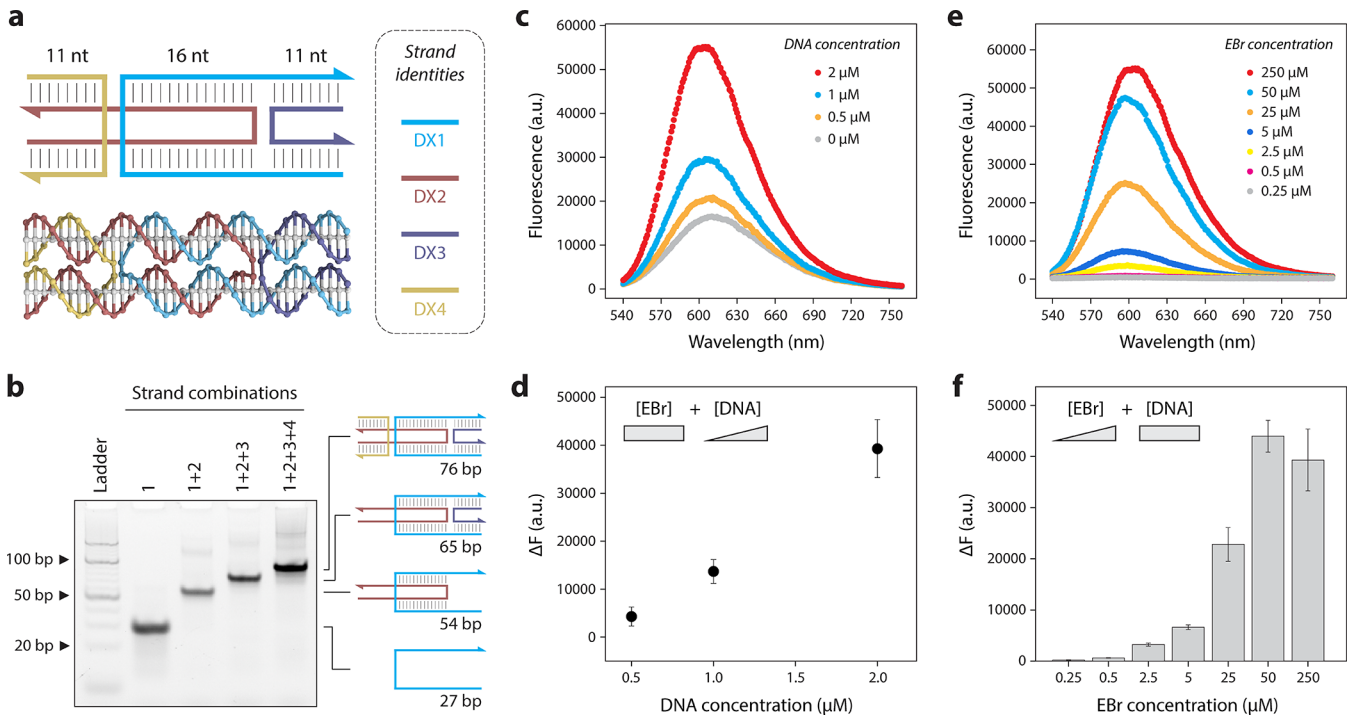

Figure 2. DX DNA-EBr complexes. (a) Design and model of the double crossover (DX) motif. (b) Nondenaturing gel showing the assembly of the DX motif. (c) Fluorescence spectra of EBr (250 μM) with different concentrations of the DX motif. (d) Differential fluorescence signals of DX/EBr complexes at 600 nm derived from the spectra shown in (c) and peak signals shown in Figure S2. (e) Fluorescence spectra of DX motif (2 μM) with different concentrations of EBr. (f) Differential fluorescence signals of DX/EBr complexes at 600 nm obtained from the spectra shown in (e) and control experiments shown in Figure S3. Data represent mean and error propagated from standard deviations of at least two experimental replicates.

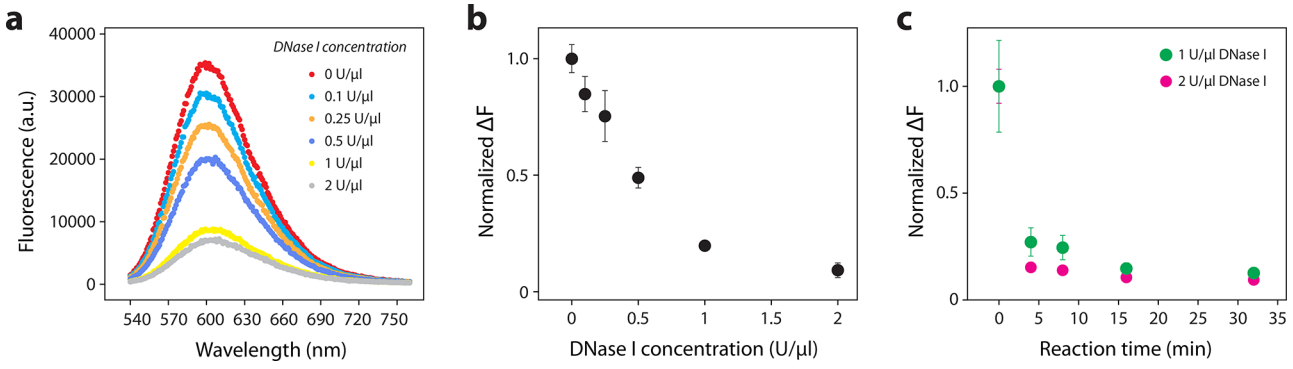

Figure 3. DNase I degradation assay for DX motif. (a) Fluorescence spectra of DX/EBr complexes treated with different concentrations of DNase I. The concentrations of the DX motif and EBr were 2 and 50 μM respectively. (b) Normalized values of differential fluorescence signals at 600 nm for different concentrations of DNase I derived from spectra shown in (a) and peak signals shown in Figure S4. (c) Normalized values of differential fluorescence signals at 600 nm for DX motif treated with 1 and 2 U/μL DNase I over different time points. Data represent mean and error propagated from standard deviations of triplicate experiments.

connected by two crossovers that are separated by 16 base pairs.[18] We assembled the DX motif by annealing the four component strands in equimolar ratios in Tris-Acetate-EDTA (TAE-Mg^{2+}) buffer and verified proper assembly using nondenaturing polyacrylamide gel electrophoresis (PAGE) (Figure 2b). We first screened different concentrations of the DX motif with EBr to obtain the optimal concentrations for fluorometric readout. We incubated 0.5, 1, and 2 μM DX motif with ~250 μM EBr and performed a fluorometric scan from 540 to 760 nm on a plate reader to obtain the fluorescence emission spectra (Figure 2c). From the spectra, we obtained the peak signal at 600 nm, which corresponded to the emission wavelength of EBr (Figure S2). We calculated the difference in fluorescence signals at 600 nm ($\Delta F = F_{[DNA+EBr]} - F_{[EBr]}$), which showed increasing signals with higher concentrations of DX motif (Figure 2d). On the basis of these results, we chose the 2 μM DNA concentration and further tested different concentrations of EBr (0.25 to 250 μM) for the best signal readout (Figure 2e). In each case, we also obtained the fluorescence spectra of EBr alone at different concentrations tested and compared the peak signals at 600 nm (Figure S3). We then calculated ΔF at 600 nm and observed an increase in fluorescence signal for up to 50 μM EBr, after which the signal decreased. The reduced fluorescence at 250 μM EBr concentration suggests that the background fluorescence of unbound EBr molecules dominates the signal at higher EBr

https://doi.org/10.1021/acsabm.3c00287
ACS Appl. Bio Mater. XXXX, XXX, XXX−XXX

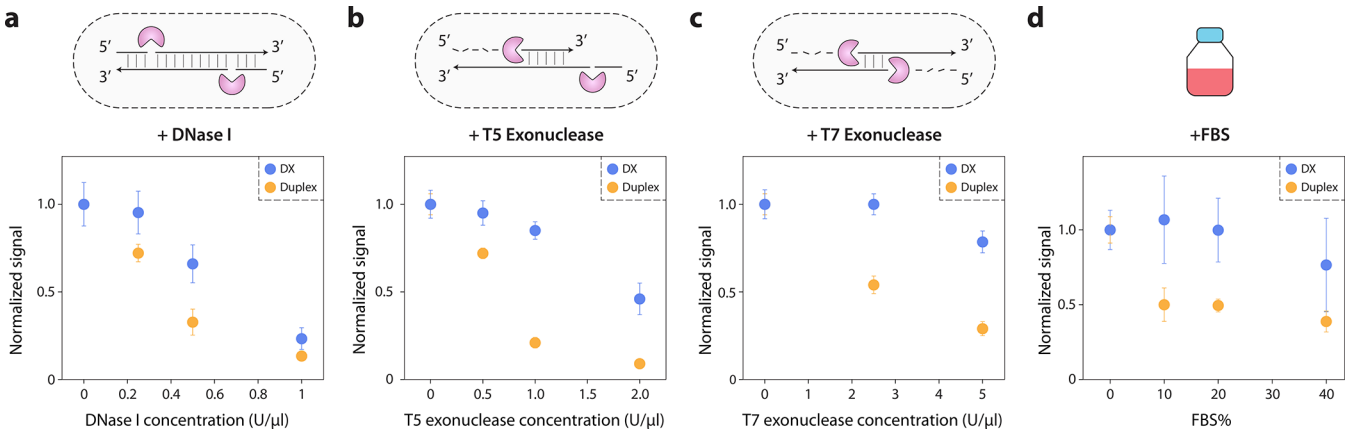

Figure 4. Biostability assay in different conditions. (a–c) Comparison of degradation profiles of duplex DNA and DX motif in different concentrations of DNase I, T5 exonuclease, and T7 exonuclease, respectively. (d) Degradation profiles of duplex and DX motif in increasing concentrations of FBS. Values are normalized to samples that had no enzyme or FBS treatment. Data represent mean and error propagated from standard deviations of triplicate experiments.

concentration ranges.[19] We selected 50 μM EBr for further experiments because it showed the highest ΔF before saturation (Figure 2f).

To demonstrate the EBr-based DNA nanostructure degradation assay, we tested the degradation of the DX motif with different concentrations of DNase I. We prepared DX/EBr complexes at the previously optimized concentrations of 2 and 50 μM, respectively, followed by incubation with 0.1, 0.25, 0.5, 1, or 2 U/μL of DNase I at 37 °C for 1 h. We obtained the fluorescence spectra for the samples and quantified the peak signal at 600 nm (Figure 3a and Figure S4). We calculated and normalized the differential fluorescence signal (ΔF) to the untreated DX and observed decreasing signal intensities with higher amounts of DNase I (Figure 3b). This indicated that the DX motif is more digested in higher amounts of the nuclease and causes release of the bound EBr. To confirm that the change in fluorescence signal is because of the release of EBr after DNA nanostructure degradation and not because of an unwinding of the DNA helix, we measured the signal of the DX/EBr complex (without any nuclease) at different time intervals for up to 2 h, which showed that the signal remains constant (Figure S5). We also performed the assay using gel electrophoresis, which showed similar degradation trends compared with the EBr-based assay (Figure S6). To further demonstrate the assay, we obtained the kinetics of the nuclease degradation reaction. We incubated the DX/EBr complex with 1 or 2 U/μL DNase I and measured the signal at 600 nm over different time points. We observed a rapid decrease in signal intensity at both DNase I concentrations, with the higher enzyme concentration degrading the structure more quickly (Figure 3c).

Next, we performed nuclease degradation experiments for a duplex DNA and compared it with the DX motif in three different nucleases: DNase I, T5 exonuclease, and T7 exonuclease (Figure 4a–c and Figure S7). We prepared duplex/EBr and DX/EBr complexes and treated the complexes with different amounts of the nucleases for 1 h at 37 °C. We obtained the fluorescence spectra and peak signals, which showed that the DX is more biostable compared with the duplex in all three enzymes. This enhanced biostability is because of the presence of crossovers in the structure, a feature we reported in our previous study for a different DX motif.[8] To demonstrate the broader applicability of the assay, we then measured degradation of the DX motif in fetal bovine serum (FBS). We incubated the DX/EBr complex in 10–40% FBS for 1 h at 37 °C and obtained the fluorescence signal at 600 nm. We also confirmed that the different serum percentages do not affect the background fluorescence signal of EBr (Figure S8). We used these background measurements to obtain ΔF between the DNA/EBr complexes and EBr alone, as well as to show that the presence of complex biological fluids does not affect the assay. With increasing serum percentages, we observed a reduction in signal intensity, thereby indicating that the DX motif is more degraded in higher serum content (Figure 4d). Higher degradation in higher percentages of FBS is possibly due to the increased levels of nuclease activity in the FBS.[6] Similar to the results from the nuclease experiments, the DX showed a higher biostability than duplex DNA in FBS.

Next, we validated the assay for DNA nanostructures of a larger size or molecular weight range by choosing a DNA origami triangle as a model nanostructure (Figure 5a). We assembled the triangle origami by mixing a circular M13 scaffold DNA and staple strands in a 1:5 ratio and annealing the mixture in TAE-Mg^{2+} buffer. We confirmed proper assembly of the triangle origami using agarose gel electrophoresis and observed results consistent with earlier reports for this structure (Figure 5b).[20] We then incubated the DNA origami structure with 50 μM EBr as we did for earlier experiments, followed by treatment with different concentrations of DNase I (Figure 5c). We observed similar trends for the DNA origami, with higher levels of degradation with increasing concentrations of DNase I.

To verify any possible effect of the intercalator on nuclease activity, we performed the nuclease degradation analysis on DX samples without EBr, followed by EBr addition for signal readout (instead of treating DX/EBr complexes). We observed slight differences in the rates of nuclease degradation but similar overall trends in both cases (Figure S9), thereby showing that for small motifs, such as the DX tested here, nuclease degradation profiles are similar in the presence of intercalators such as EBr. To demonstrate the adaptability of the assay to other fluorescent intercalators, we performed a similar nuclease degradation assay for the DX motif using GelRed, a nontoxic alternative to EBr, and obtained comparable results (Figure S10).

https://doi.org/10.1021/acsabm.3c00287
ACS Appl. Bio Mater. XXXX, XXX, XXX–XXX

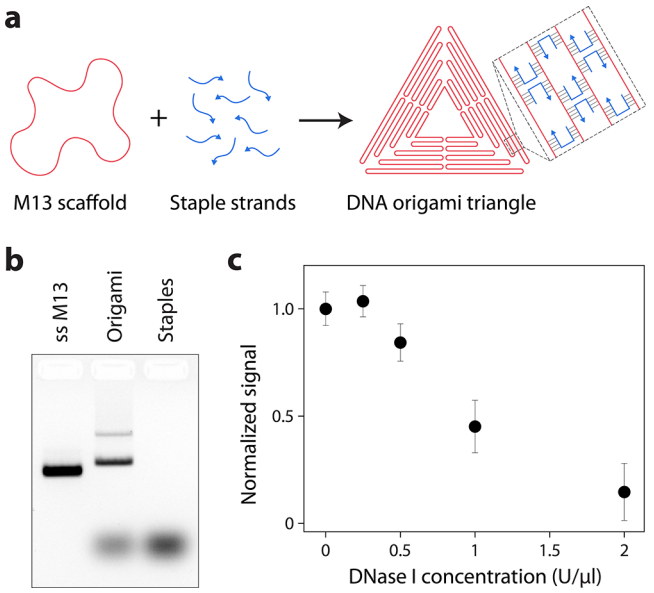

Figure 5. DNase I degradation assay for DNA origami. (a) Schematic of DNA origami assembly. (b) Agarose gel analysis of DNA origami assembly. (c) Degradation of DNA origami in different concentrations of DNase I. Data represent mean and error propagated from standard deviations of triplicate experiments.

In summary, we present an intercalator-based fluorescence assay to analyze degradation of DNA nanostructures against nucleases and in biofluids. This assay allows the evaluation of multiple samples of DNA nanostructures using a plate reader, with rapid readout of peak emission signals for the type of intercalator used. This is an advantage compared with other characterization methods where the readout takes hours and can be limited to fewer samples (Table S1). While gel-based analysis is more frequently used, there are still some challenges associated with the method. For example, in DNA nanostructures containing cationic block copolymers, the nanostructures need to be decomplexed from the copolymers before they can be analyzed on a gel.[21] Moreover, in studies involving biofluids, the serum proteins could cause a background signal in both gel electrophoresis and TEM analysis.[1] When compared with other fluorescence readout methods, the method presented here provides a cheaper alternative to using fluorophore-labeled oligonucleotides. This assay can also be used for larger DNA nanostructures, as demonstrated by the DNA origami results. Further, the method is readily adaptable for use with other fluorescent intercalators with minimal optimization. The method could also be used to analyze the biostability of RNA or hybrid DNA/RNA nanostructures against ribonucleases. We further show that the assay works well in biofluids, such as bovine serum, with minimal to no difference in background fluorescence signal.

Our assay also has some limitations. Similar to gel electrophoresis and fluorophore-based techniques, this method provides the degradation levels of nanostructures but not details on structural changes. Since the method uses an intercalating dye bound to DNA nanostructures, differences in binding of the dye to such structures may also play a role in the assay. While some studies have shown that the nanostructure design affects the intercalation of small molecules (such as steric or electrostatic effects due to the proximity of the helices in DNA origami[22] and different binding modes in corners of polyhedra[23]), recent studies on intercalators bound to different DNA origami structures[24] have shown that there are minimal differences in the intercalation of such small molecules in different structures. Since most nuclease degradation profiles are normalized to undamaged or untreated samples, any such difference in intercalator binding might only cause a minimal effect in the results. In a previous study, intercalators have been shown to confer additional biostability to large DNA origami nanostructures (doxorubicin in that case).[24] In our control experiment with DNase I, we observed similar degradation trends for the DX motif in the presence or absence of EBr, thereby showing that presence of intercalators in such small DNA motifs has minimal effect on the assay. In methods such as gel electrophoresis, typically, the band corresponding to the DNA nanostructure is quantified to analyze degradation (reduction in band intensities), which indicates the fraction of intact structures. In the intercalator-based assay reported here, the results typically indicate the amount of intercalator molecules bound to the DNA nanostructures at different time points or in different solution conditions. This provides a rather indirect analysis of DNA nanostructure degradation since EBr molecules may still be bound to degraded DNA nanostructures. Thus, there might still be a remnant signal even if the DNA nanostructure is no longer fully intact but is also not fully digested by the nucleases.

Overall, this method could be a useful alternative to or complement other methods that analyze the nuclease degradation profiles (or enhanced nuclease resistance) of DNA nanostructures. With the variety of conditions being explored for DNA nanostructure assembly, this method provides a simple, high-throughput workflow for analyzing the biostability of DNA nanostructures in different physiological conditions.

■ ASSOCIATED CONTENT

Supporting Information

The Supporting Information is available free of charge at https://pubs.acs.org/doi/10.1021/acsabm.3c00287.

Methods, additional experimental results, and oligonucleotide sequences used (PDF)

■ AUTHOR INFORMATION

Corresponding Author

Arun Richard Chandrasekaran − *The RNA Institute, University at Albany, State University of New York, Albany, New York 12203, United States;* orcid.org/0000-0001-6757-5464; Email: arun@albany.edu

Authors

Hannah Talbot − *The RNA Institute, University at Albany, State University of New York, Albany, New York 12203, United States*

Bharath Raj Madhanagopal − *The RNA Institute, University at Albany, State University of New York, Albany, New York 12203, United States;* orcid.org/0000-0003-1043-8754

Andrew Hayden − *The RNA Institute, University at Albany, State University of New York, Albany, New York 12203, United States*

Ken Halvorsen − *The RNA Institute, University at Albany, State University of New York, Albany, New York 12203, United States;* orcid.org/0000-0002-2578-1339

Complete contact information is available at: https://pubs.acs.org/10.1021/acsabm.3c00287

https://doi.org/10.1021/acsabm.3c00287
ACS Appl. Bio Mater. XXXX, XXX, XXX−XXX

Author Contributions

H.T. performed experiments and analyzed data; B.R.M. analyzed data and edited the manuscript; A.H. performed experiments; K.H. supervised the project and edited the manuscript; A.R.C. conceived and supervised the project, designed experiments, analyzed and visualized data, and wrote the manuscript. All authors provided comments on the manuscript.

Funding

Research reported in this publication was supported by the National Institutes of Health (NIH) through the National Institute on Aging (NIA) under award R03AG076599 to A.R.C. and the National Institute of General Medical Sciences (NIGMS) under award R35GM124720 to K.H.

Notes

The authors declare no competing financial interest.

REFERENCES

(1) Chandrasekaran, A. R. Nuclease Resistance of DNA Nanostructures. *Nature Reviews Chemistry* **2021**, *5* (4), 225−239.
(2) Klocke, M. A.; Garamella, J.; Subramanian, H. K. K.; Noireaux, V.; Franco, E. Engineering DNA Nanotubes for Resilience in an E. Coli TXTL System. *Synthetic Biology* **2018**, *3* (1), No. ysy001.
(3) Simmons, C. R.; Zhang, F.; MacCulloch, T.; Fahmi, N.; Stephanopoulos, N.; Liu, Y.; Seeman, N. C.; Yan, H. Tuning the Cavity Size and Chirality of Self-Assembling 3D DNA Crystals. *J. Am. Chem. Soc.* **2017**, *139* (32), 11254−11260.
(4) Kiviaho, J. K.; Linko, V.; Ora, A.; Tiainen, T.; Järvihaavisto, E.; Mikkilä, J.; Tenhu, H.; Nonappa; Kostiainen, M. A. Cationic Polymers for DNA Origami Coating − Examining Their Binding Efficiency and Tuning the Enzymatic Reaction Rates. *Nanoscale* **2016**, *8* (22), 11674−11680.
(5) Anastassacos, F. M.; Zhao, Z.; Zeng, Y.; Shih, W. M. Glutaraldehyde Cross-Linking of Oligolysines Coating DNA Origami Greatly Reduces Susceptibility to Nuclease Degradation. *J. Am. Chem. Soc.* **2020**, *142* (7), 3311−3315.
(6) Hahn, J.; Wickham, S. F. J.; Shih, W. M.; Perrault, S. D. Addressing the Instability of DNA Nanostructures in Tissue Culture. *ACS Nano* **2014**, *8* (9), 8765−8775.
(7) Wamhoff, E.-C.; Romanov, A.; Huang, H.; Read, B. J.; Ginsburg, E.; Knappe, G. A.; Kim, H. M.; Farrell, N. P.; Irvine, D. J.; Bathe, M. Controlling Nuclease Degradation of Wireframe DNA Origami with Minor Groove Binders. *ACS Nano* **2022**, *16* (6), 8954−8966.
(8) Chandrasekaran, A. R.; Vilcapoma, J.; Dey, P.; Wong-Deyrup, S. W.; Dey, B. K.; Halvorsen, K. Exceptional Nuclease Resistance of Paranemic Crossover (PX) DNA and Crossover-Dependent Biostability of DNA Motifs. *J. Am. Chem. Soc.* **2020**, *142* (14), 6814−6821.
(9) Xin, Y.; Piskunen, P.; Suma, A.; Li, C.; Ijäs, H.; Ojasalo, S.; Seitz, I.; Kostiainen, M. A.; Grundmeier, G.; Linko, V.; Keller, A. Environment-Dependent Stability and Mechanical Properties of DNA Origami Six-Helix Bundles with Different Crossover Spacings. *Small* **2022**, *18* (18), No. 2107393.
(10) Chandrasekaran, A. R.; Halvorsen, K. Nuclease Degradation Analysis of DNA Nanostructures Using Gel Electrophoresis. *Current Protocols in Nucleic Acid Chemistry* **2020**, *82*, No. e115.
(11) Goltry, S.; Hallstrom, N.; Clark, T.; Kuang, W.; Lee, J.; Jorcyk, C.; Knowlton, W. B.; Yurke, B.; Hughes, W. L.; Graugnard, E. DNA Topology Influences Molecular Machine Lifetime in Human Serum. *Nanoscale* **2015**, *7* (23), 10382−10390.
(12) Ijäs, H.; Liedl, T.; Linko, V.; Posnjak, G. A Label-Free Light-Scattering Method to Resolve Assembly and Disassembly of DNA Nanostructures. *Biophys. J.* **2022**, *121* (24), 4800−4809.
(13) Ramakrishnan, S.; Shen, B.; Kostiainen, M. A.; Grundmeier, G.; Keller, A.; Linko, V. Real-Time Observation of Superstructure-Dependent DNA Origami Digestion by DNase I Using High-Speed Atomic Force Microscopy. *ChemBioChem.* **2019**, *20* (22), 2818−2823.
(14) Zagorovsky, K.; Chou, L. Y. T.; Chan, W. C. W. Controlling DNA−Nanoparticle Serum Interactions. *Proc. Natl. Acad. Sci. U.S.A.* **2016**, *113* (48), 13600−13605.
(15) Langlois, N. I.; Clark, H. A. Characterization of DNA Nanostructure Stability by Size Exclusion Chromatography. *Anal. Methods* **2022**, *14* (10), 1006−1014.
(16) Halvorsen, K.; Kizer, M. E.; Wang, X.; Chandrasekaran, A. R.; Basanta-Sanchez, M. Shear Dependent LC Purification of an Engineered DNA Nanoswitch and Implications for DNA Origami. *Anal. Chem.* **2017**, *89* (11), 5673−5677.
(17) Olmsted, J. I.; Kearns, D. R. Mechanism of Ethidium Bromide Fluorescence Enhancement on Binding to Nucleic Acids. *Biochemistry* **1977**, *16* (16), 3647−3654.
(18) Fu, T. J.; Seeman, N. C. DNA Double-Crossover Molecules. *Biochemistry* **1993**, *32* (13), 3211−3220.
(19) Madhanagopal, B. R.; Chen, S.; Platt, C.-D.; Chandrasekaran, A. R. Caffeine-Induced Release of Small Molecules from DNA Nanostructures. *iScience* **2023**, *26* (5), 106564.
(20) Jiang, Q.; Song, C.; Nangreave, J.; Liu, X.; Lin, L.; Qiu, D.; Wang, Z.-G.; Zou, G.; Liang, X.; Yan, H.; Ding, B. DNA Origami as a Carrier for Circumvention of Drug Resistance. *J. Am. Chem. Soc.* **2012**, *134* (32), 13396−13403.
(21) Agarwal, N. P.; Matthies, M.; Gür, F. N.; Osada, K.; Schmidt, T. L. Block Copolymer Micellization as a Protection Strategy for DNA Origami. *Angew. Chem., Int. Ed.* **2017**, *56* (20), 5460−5464.
(22) Miller, H. L.; Contera, S.; Wollman, A. J. M.; Hirst, A.; Dunn, K. E.; Schröter, S.; O'Connell, D.; Leake, M. C. Biophysical Characterisation of DNA Origami Nanostructures Reveals Inaccessibility to Intercalation Binding Sites. *Nanotechnology* **2020**, *31* (23), 235605.
(23) Xu, Y.; Huang, S.; Ma, Y.; Ding, H. Loading of DOX into a Tetrahedral DNA Nanostructure: The Corner Does Matter. *Nanoscale Adv.* **2022**, *4* (3), 754−760.
(24) Ijäs, H.; Shen, B.; Heuer-Jungemann, A.; Keller, A.; Kostiainen, M. A.; Liedl, T.; Ihalainen, J. A.; Linko, V. Unraveling the Interaction between Doxorubicin and DNA Origami Nanostructures for Customizable Chemotherapeutic Drug Release. *Nucleic Acids Res.* **2021**, *49* (6), 3048−3062.

https://doi.org/10.1021/acsabm.3c00287
ACS Appl. Bio Mater. XXXX, XXX, XXX−XXX